Comparison between FBP and SART for digital tomosynthesis for PCB inspection

Jonghee Yun [a], Junbeom Park [a], Seungwoo Ha [a], Ho Kyung Kim [a,b*]
[a]*School of Mechanical Engineering, Pusan National University, Busan, South Korea*
[b]*Center for Advanced Mechanical Engineering Research, Pusan National University, Busan, South Korea*
[*]*Corresponding author: hokyung@pusan.ac.kr*

1. Introduction

Digital tomosynthesis (DTS) is a technique for acquiring images from a limited view angles, while it is not fully sampled in the Fourier space, resulting in insufficient data for image reconstruction. Nonetheless, there are image reconstruction algorithms such as filtered backprojection (FBP), simultaneous algebraic reconstruction technique (SART), and compressed sensing (CS) that can reconstruct images with insufficient data. These algorithms have advantages and disadvantages in image quality and reconstruction speed.

In the study, we compare the tomosynthesis images reconstructed using FBP and SART.

2. Materials and Methods

2.1 Image reconstruction algorithms

The image reconstruction algorithms used in this study are FBP and SART. The FBP algorithm is the most commonly used algorithm for CT image reconstruction. Since it can calculate slice images analytically, it can provide accurate and fast results. However, when reconstructing the image using the FBP algorithm with data obtained from a limited angle, there have been reported that several Fourier domain artifacts during the filtering process could occur. On the contrary, the SART algorithm is a method of reconstructing images by iteratively obtaining solutions of algebraic equations. Therefore, the SART algorithm can avoid the Fourier domain artifacts. However, since the image is reconstructed iteratively, the complexity of the calculation becomes a problem.

2.2 Filtered Backprojection

The most commonly used image reconstruction algorithm is the FBP algorithm. The FBP algorithm approximates the backprojection procedure of cone beam geometry to parallel beam geometry. The FBP algorithm can be represented by following equation [1].

$$f(r)=\int_{\beta_{\min}}^{\beta_{\max}} d\beta \frac{L^2}{(\lambda-\mathrm{r}\bullet(\mathrm{n}_{\xi}\times\mathrm{n}_{\eta}))^2}\left[\tilde{p}_{\beta}(\xi,\eta)*h(\xi)\right], \quad (1)$$

where L is the distance from source to detector, λ is the distance from source to rotation center, and $f(r)$ is

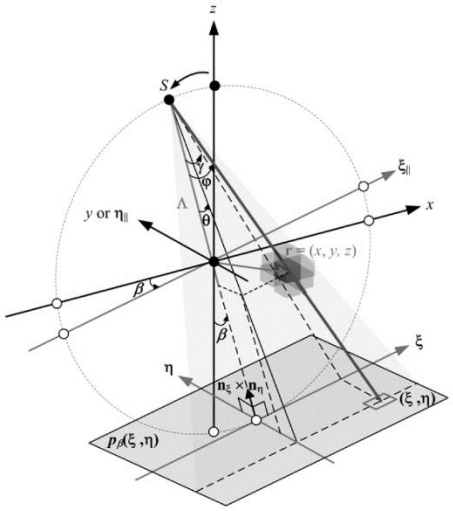

Fig. 1. A sketch describing image reconstruction in cone beam geometry. To reconstruct voxel value at $=(x,y,z)$, the contribution of projection value at (ξ,η) in the planar detector obtained at the projection angle β is illustrated. The projection signal is backprojected along the line, which is contained in the tilted fan beam [4].

an object function in spatial coordinate. $\tilde{p}_{\beta}(\xi,\eta)$ means the projection image multiplied by weighting factor:

$$\tilde{p}_{\beta}(\xi,\eta)=\frac{L}{\sqrt{L^2+\xi^2+\eta^2}}\,p_{\beta}(\xi,\eta)\,, \quad (2)$$

The weighting function defined in equation (1) makes approximately cone beam to parallel beam geometry. $h(\xi)$ in equation (1) refers to the filter function. The integral operation means the backprojection [4].

In cone beam computed tomography (CBCT) image reconstruction, the calculation of the backprojection indicates the existence of a transfer function that is inversely proportional to frequency. Therefore, an inverse transfer function is needed to compensate the loss. This inverse function is the filter function h. This filter function can be described by the following equation in the spatial frequency domain.

$$H_{RA}(u,v)=\beta_{scan}\sqrt{u^2+v^2}\,, \quad (3)$$

The ramp filter compensates the low frequency data. However, it amplifies noise in high frequency data. To minimize high frequency noise, we use Hann window function as apodization filter. Hence this filter is called spectral apodizing as Lauritsch and Härer [3, 4].

In DTS, it requires an additional filter. The DTS obtains data in limited angular ranges. Therefore, deficiencies of data occur along w-direction, which is perpendicular to detector plane (u, v). This causes blur artifact. In order to reduce this artifact, we use the Hann window, which is the same filter as spectral apodizing filter. This is called the slice thickness filter [3].

2.3 Simultaneous algebraic reconstruction technique

In digital tomosynthesis imaging, there are many missing data, which makes the accurate image reconstruction more difficult, because of the limited view angle. Therefore, iterative image reconstruction technique is used to estimate the original object. The SART is one of the most commonly used iterative image reconstruction techniques. The SART updates in projection by projection at each iteration. A 3D image is updated with SART reconstruction by using the following formation [2].

$$g_j^{(k+1)} = g_j^{(k)} + \frac{\sum_i \left[a_{ij} \frac{p_i - \vec{a}_i^T \vec{g}^{(k)}}{\sum_{j=1}^{N} a_{ij}} \right]}{\sum_i a_{ij}}, \quad (4)$$

where the coefficients a_{ij} represent the net effect of the linear transformations, p shows the measured projected data, and g is the image to be reconstructed, *i* and *j* are ray and voxel indexes respectively.

2.4 Comparison metrics

To compare the images reconstructed with FBP with those reconstructed with SART, we investigate the similarity of images using structural information (SSIM) and mutual information (MI). SSIM is used for measuring the similarity between two images. SSIM is given by [5]

$$\mathrm{SSIM}(x,y) = \frac{(2\mu_x\mu_y + C_1)(2\sigma_{xy} + C_2)}{(\mu_x^2 + \mu_y^2 + C_1)(\sigma_x^2 + \sigma_y^2 + C_2)}, \quad (5)$$

where μ_x and μ_y are the average of x and y, respectively. σ_x^2 and σ_y^2 are the variance of x and y, respectively. σ_{xy} is the covariance of x and y. And C_1 and C_2 are variables to stabilize the division with weak denominator, which is defined as $(k_1 L)^2$ and $(k_2 L)^2$, respectively. Where L is the dynamic range of the pixel-values, and k_1 and k_2 are 0.01 and 0.03 by default, respectively.

MI measures the mutual dependence between the two images. The MI can be defined by [6]

$$I(X;Y) = \sum_{y \in Y} \sum_{x \in X} p(x,y) \log 2 \left(\frac{p(x,y)}{p(x)p(y)} \right), \quad (6)$$

where $p(x,y)$ is the joint probability distribution function of X and Y, and $p(x)$ and $p(y)$ are the marginal probability distribution function of X and Y, respectively.

2.5 Experimental phantom

To compare the reconstructed images from the FBP and SART algorithms, we used the PCB used in the automobile LED as an experimental phantom as shown in Fig. 2.

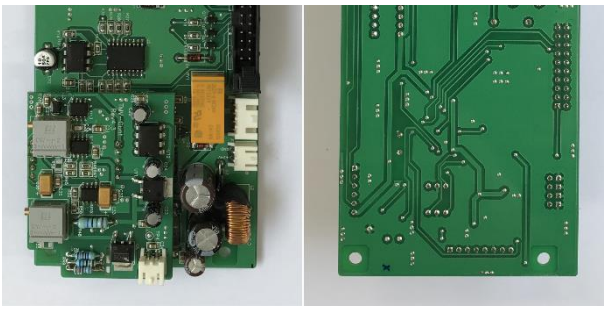

Fig. 2. LED PCB to reconstruct. (a) front of PCB. (b) back of PCB

3. PRELIMINARY RESULT

Fig. 3 shows the reconstructed slice images of LED PCB phantom depicted in Fig. 2 by using the FBP and the SART algorithms. The projection images are taken from angular range of 30°. Fig. 3(a) and (b) are obtained using the FBP algorithm. And Fig. 4 is obtained using the SART algorithm. Fig. 4(a) and (b) are obtained by 5 iteration, Fig. 4(c) and (d) are obtained by 10 iteration, and Fig. 4(e) and (f) are obtained by 15 iteration.

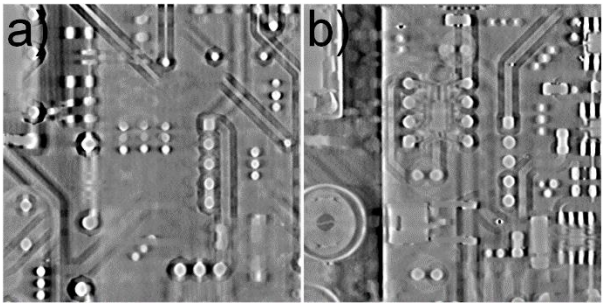

Fig. 3. Reconstructed slice images of LED PCB phantom by using the FBP algorithm.

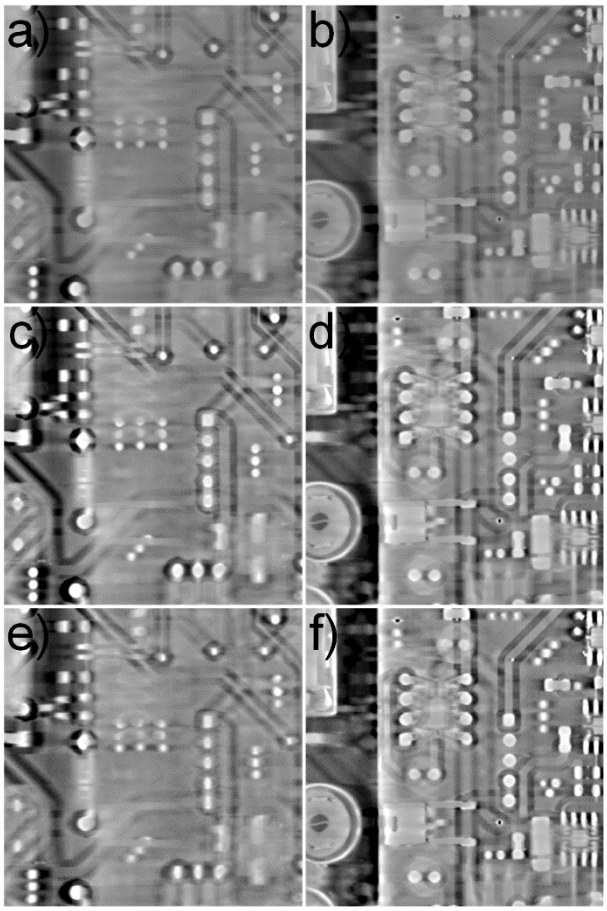

Fig. 4. Reconstructed slice images of LED PCB phantom by using the SART algorithm.

4. FURTHER STUDY

We have designed multi-layered PCBs, which contains quantitative information. Quantitative analysis on the reconstructed images for the phantoms will be performed by using the SSIM and MI metrics.

ACKNOWLEDGEMENT

This work was supported by the National Research Foundation of Korea (NRF) grant funded by the Korea government (MSIP) (No. 2013M2A2A9046313).

REFERENCES

[1] L. A. Feldkamp, L. C. Davis, and J. W. Kress, Practical cone-beam algorithm, *J. Opt. Soc. Am. A.*, Vol. 1, pp. 612-619, 1984.
[2] A. C. Kak and M. Slaney, Principles of computed tomography imaging, IEEE press, New York, 1988.
[3] G. Lauritsch and W. H. Härer, Theoretical framework for filtered back projection in tomosynthesis, *Proc. SPIE*, Vol. 3388, pp. 1127-1137, 1998
[4] H. Youn, J. S. Kim, M. K. Cho, S. Y. Jang, W. Y. Song, and H. K. Kim, Optimizing imaging conditions in digital tomosynthesis for image-guided radiation therapy, *Korean J. Med. Phys.*, Vol. 21, pp. 281-290, 2010.
[5] Z. Wang, A. C. Bovik, H. R. Sheikh, E. P. Simoncelli, Image quality assessment: From error measurement to structural similarity, IEEE Trans. Image Process., vol. 13, no. 4, pp. 600-512, Apr. 2004.
[6] Cover, Thomas M., and Joy A. Thomas. Elements of information theory. John Wiley & Sons, 2012.